THERMAL PROPERTY OF SELF-CROSS-LINKING SILK FIBROIN SCAFFOLDS

by

Yu LIU[a,b*], Li-Fen CHEN[b], Jian-Hua SUI[a], Xiu-Ming CAO[b], Yiao-Ying DING[b], and Ming-Zhong LI[a]

[a] National Engineering Laboratory for Modern Silk, College of Textile and Clothing Engineering, Soochow University, Suzhou, China
[b] Jiangsu Sunshine Group, Jiangyin, Jiangsu, China

Original scientific paper
https://doi.org/10.2298/TSCI2303165L

Thermal property of the silk fibroin scaffolds has triggered rocketing interest in tissue engineering because it affects greatly the scaffolds reliability and efficiency. This paper suggests a promising method to optimize the scaffolds by a tyrosinase-catalyzed self-cross-linking reaction, the effects of tyrosinase concentrations on scaffolds thermal and physical properties are studied experimentally. The enzymatic cross-linking offers a new and promising angle for preparation of SF materials.

Key words: *silk fibroin, tyrosinase, self-cross-linking, pore structure*

Introduction

Silk fibroin (SF) has been utilized in biomaterials for tissue engineering and regenerative medicine due to its excellent biocompatibility, low immunogenicity, and stable mechanical properties [1]. Depending on different preparation methods, *e.g.* the electrospinning method [2] or the bubble electrospinning method [3], SF can assume several forms, *e.g.*, sponge, nanofiber mesh, films, and hydrogel, for various biomedical applications [4], which lead to different mechanical and biological properties [5]. Even though known as biocompatibility, the regenerated SF materials without cross-linking display poor mechanical properties, which limit its application in biomedical materials. Moreover, the processing conditions of cross-linking will influence the characteristics of the regenerated SF materials, such as the secondary structure, molecular weight, amino acid composition and so on [6], and surface morphology as discussed in [7], and in turn, its biocompatibility and biodegradation will be greatly affected. Too slow or quick degradation rate in vivo does not meet the demand of tissue engineering applications [8]. To solve these problems, a variety of cross-linking methods were used to manufacture regenerated SF materials. Common physical cross-linking methods, such as high temperature, organic solvent, or metal ion treatments, can improve the water resistance of the material [9] especially for those with hierarchical structure [10]. However, its mechanical strength and stability are usually insufficient [11], for example a nanoscale membrane [12] can not resist a large external force. The chemical cross-linking agents, including glutaraldehyde, carbodiimide, diglycidyl and so on, would induce a covalent bond between the intra- and inter-molecules to form a network structure, which improves the stability and flexibility of materials [13, 14]. Although chemical cross-linking reduces water-soluble de-

* Corresponding author, e-mail: liuyu@suda.edu.cn

gree and improves the mechanical properties of materials, the residual chemicals would damage material biocompatibility or cause environmental pollution [15]. Furthermore, some chemical reactions are full of shortcomings in complicated reaction steps or low reaction yield [16]. So, it is desirable to seek a new simple cross-linking method which would maintain biocompatibility and modulate structure of regenerated SF materials.

These limitations of common cross-linking methods can be overcome by using enzymes to form cross-linked materials. Enzymes can functionalize biopolymers to production of novel functions or alter structural properties. Biopolymers containing phenolic compounds, such as proteins, polysaccharides or lignin, can be oxidized by enzymes (*e.g.* transglutaminase, phosphatases, thermolysin, tyrosinase) and the oxidation reactions will lead to a cross-linking. Tyrosinase, known as phenoloxidase and monophenol monooxygenase, is widely distributed in microorganisms, plants, animals, and the human body [17]. It can oxidize various phenolic compounds and result in a cross-linking formation. Tyrosine side chains in proteins contain phenolic hydroxyl can be oxidized by tyrosinase [18].

The SF contains tyrosine in semicrystalline or amorphous region, and the content of this aromatic amino acid is about 10-12 mol.% [19], so the use of enzymatic cross-linking for preparation of SF materials is an alternative promising choice. In this study, the tyrosinase-catalyzed self- cross-linking SF (c-SF) scaffolds with varying reaction ratios of tyrosinase against SF (TYR/SF) were constructed to investigate the influence of TYR/SF ratios on the structure of c-SF scaffolds, which are important requirements of supporting matrixes intended for tissue engineering field.

Experimental design

Bombyx mori raw silk fibers were purchased from Zhejiang Second Silk Co. Ltd. (Huzhou, China). Tyrosinase extracted by mushroom (T3824-25KU) were purchased from Sigma-Aldrich (Germany). All other chemicals were analytical grade and purchased from Sinopharm Chemical Reagent Co. Ltd. (Shanghai, China).

Silk fibers were degummed three times with 0.05% (w/w) Na_2CO_3 solution at 98 ℃ for 30 minutes and rinsed thoroughly and dried in oven at 60 ℃. The extracted silk was dissolved in $CaCl_2/H_2O/CH_3CH_2OH$ solution at 70 ±2 ℃ for 1 hour, and then dialyzed in deionized water for 72 hours to yield SF aqueous solution. The concentration of SF solution was 1.0, 2.0, and 3.0%, respectively. Then the tyrosinase powder was added into the SF solution, and the final reaction ratios of tyrosinase against SF in mixed solution were 1/6000, 1/3000, 1/2000, 1/1500, 1/1200, 1/600, and 1/300, respectively. Subsequently, the reaction proceeded for 90 minutes by mixing the solution at 25 ±2 °C. Finally, the mixture solution was casted into a petri dish and freeze-dried to obtain t-SF scaffolds with varying reaction SF concentration.

The c-SF scaffolds were dissolved in distilled water (bath ratio 1:30) after the equilibration of 1 hour, and then mixed with the ninhydrin aqueous solution (0.1% w/v) and stirred slowly in water bath at 100 °C ±2 °C for 20 minutes. After centrifugation, the optical density (OD) value of the supernatant at 570 nm was obtained by using an ultraviolet spectrophotometer (Hitachi, UV-3010). The cross-linking degree was expressed as the percentage of reacted free amine number relative to the initial free amine number. Then the SF scaffolds with different TYR/SF ratios were prepared by hydrolysis in 6 M hydrochloric acid at 110 ±1 °C for 22 hours. The amino acid analyzer (Hitachi, L-8900) was used to determine the identity and quantity of amino acids in the hydrolyzed products.

The c-SF scaffolds were dried in a vacuum oven at 105 ±2 °C. The moisture weight of the sample was m_1, while the moisture weight fraction, w, is defined as the ratio of the mass

of water to the mass of fully dried c-SF scaffolds. Then the c-SF scaffolds were immersed into distilled water (bath ratio 1:100) in a beaker maintaining a mild agitation at 37 ±2 °C for 24 hours. The undissolved fraction of the c-SF scaffolds was fully dried under the same condition and its weight was m_2. The hot-water-solubility degree was calculated from the equation: hot water-solubility degree = $[1 - m_2/(m_1 - m_1 w)]$.

The cross-sectional morphology of porous c-SF scaffolds was observed by Hitachi S-4800 SEM. The border of each pore in top layer was defined according to gradient method. Thus their pictures of the top layer of their cross sections were obtained. Each pore area x_1, x_2, …, x_n and the area, S, of porous c-SF scaffolds material in statistic range, were calculated according to the limits of each pore in bmp and the number of picture points in the whole picture. And the average pore diameter, $\bar{d}$, was given by:

$$\bar{d} = \frac{\left(\sum_{i=1}^{n} \sqrt{\frac{4x_i}{\pi}}\right)}{n}$$

The X-ray diffraction was performed by X'Pert-Pro MPD (Holland) diffractometer, and CuKα radiation with a wavelength of 1.5406 Å was used. The scanning speed was 2° per mm. The diffraction intensity curves with 2θ from 5° to 45 °were obtained.

Results and discussion

Cross-linking degree reflected the extent of reaction between free amino side chains of SF and tyrosine residues oxidized by tyrosinase. The results shown in fig. 1 demonstrated that cross-linking degree of the c-SF scaffolds was 54% when the reaction ratio of tyrosinase against SF (TYR/SF) was 1/6000. The increase of the reaction ratios of TYR/SF from 1/3000 to 1/2000 resulted in a significant increase of the cross-linking degree from 63% to 86%. Furthermore, growth of cross-linking degree became slow and stable, and the stable cross-linking degree was about 88% when the TYR/SF ratios reached 1/300. This phenomenon was due to the decrease of the free amino groups of SF in the reaction process. It indicated that the cross-linking degree of SF scaffolds could be adjusted by the reaction ratios of TYR/SF. The result further proved the cross-linking reaction were occurred, and the tyrosinase was the target of the tyrosinase-catalyzed cross-linking reaction system, see tab. 1.

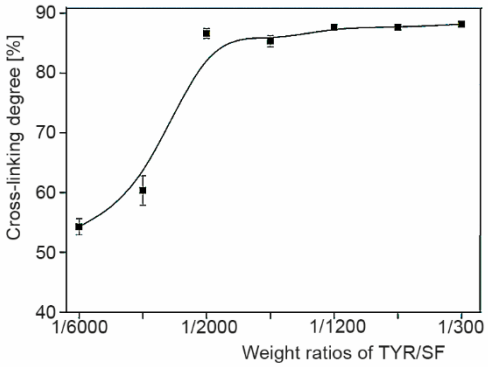

Figure 1. Effect of TYR/SF ratios on cross-linking degree of c-SF scaffolds

The hot water-solubility degree reflected the thermal stability of SF scaffolds after cross-linking. The results in fig. 2 showed that the increase of TYR/SF ratio from 1/6000 to 1/3000 and 1/2000 resulted in a significant decrease of the hot water-solubility degree from 38% to 24%, and 13%. When the TYR/SF ratio was 1/300, it was only 8%. It revealed that c-SF scaffolds performed a better water tolerance ability after tyrosinase-catalyzed cross-linking by adjusting the reaction ratios of TYR/SF. The c-SF scaffolds with TYR/SF ratios of 1/300 were selected to investigation in future study.

Table 1. Amino acid composition of un-cross-linked SF scaffolds and c-SF scaffolds [mol.%]

Amino acid	Type of SF scaffolds		
	Un-cross-linked SF scaffolds	c-SF scaffolds (TYR/SF = 1/3000)	c-SF scaffolds (TYR/SF = 1/300)
Ser	11.81 ±0.12	11.14 ±0.10	11.05 ±0.13
Gly	44.63 ±0.15	45.07 ±0.31	45.44 ±0.18
Ala	30.35 ±0.23	31.12 ±0.09	31.46 ±0.26
Val	2.24 ±0.03	2.15 ±0.29	2.24 ±0.22
Tyr	10.16 ±0.02	8.16 ±0.04	7.35 ±0.12
others	0.81 ±0.06	1.91 ±0.06	2.46 ±0.13

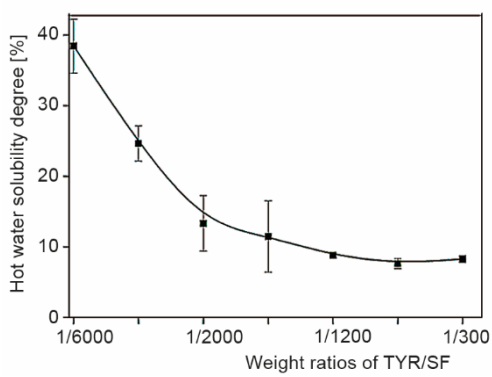

Figure 2. Effect of TYR/SF ratios on hot water-solubility degree of c-SF scaffolds

Figure 3 showed the influence of SF concentration on c-SF scaffold structure. The pore shape of the low concentration c-SF scaffold was anomalous, 1%, fig. 3(a), and the pore size was 101.47 ±23.68 μm, tab. 2. With the increasing of the proportion of SF concentration, the pore shape gradually changed to fusiform, and the pore size reduced to 91.21 ±13.99 μm for 2% SF concentration, fig. 3(b). When the SF concentration was 4%, the pore shape was almost fusiform and pore size was 46.40 ±10.37 μm, fig. 3(d).

The reason might be that SF solution was concentrated and gathered when the ice particles grew. From fig. 3 and tab. 2, we could see that the average pore size of c-SF scaffolds was 46-101 μm, and the higher the proportion of SF concentration, the smaller pore size. In general, the pore size is dependent on the size of ice particles, and the ice particles size is closely related with the solution concentration. The high concentration was not favorable to the formation of large ice particles. During the freeze-drying process, the porous materials would have different degree of contraction. With the increasing of the proportion of SF concentration, the degree of contraction become greater, so the pore size of scaffolds is smaller. Therefore, the pore shape and pore size of c-SF scaffolds may be regulated by adjusting the reaction SF concentration.

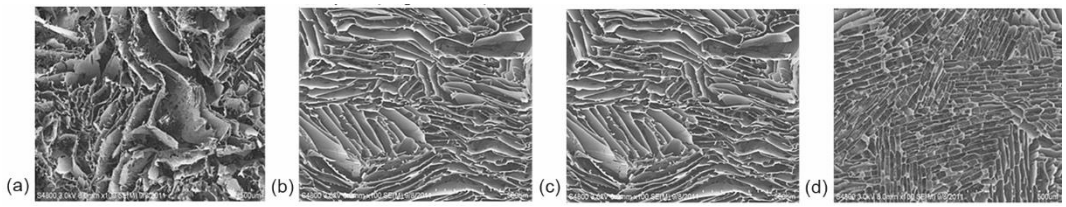

Figure 3. The SEM images of c-SF scaffolds with different reaction SF concentration; (a) 1%, (b) 2%, (c) 3%, and (d) 4%

Table 2. Influence of reaction SF concentration on the pore size and porosity

Sample	a	b	c	d
Pore size [μm]	101.47 ±23.68	91.21 ±13.99	73.09 ±16. 13	46.40 ±10.37
Porosity [%]	60.26	56.39	47.51	41.63

The curve of c-SF scaffold (1%) shows a comparative major peak at around 20.2° in XRD curve, the curve a in fig. 4(a), indicating that the inside condensed structure is mainly random coil and contains a few α-structure. From the XRD curve of c-SF scaffolds, with the increasing of the proportion of SF concentration, the significant scattering diffraction peak at 20.2°, did not change, demonstrating that the crystal structure did not change with the increasing reaction SF concentration. The exothermic peak of c-SF scaffold near 219 ℃ and 286 ℃ regardless of SF concentration from DSC curve, fig. 4(b), and the thermal decomposition temperature of the material after cross-linking did not change significantly. It means that the condensed structure is mainly random coil and contains a few α-structure, which were consistent with results of XRD.

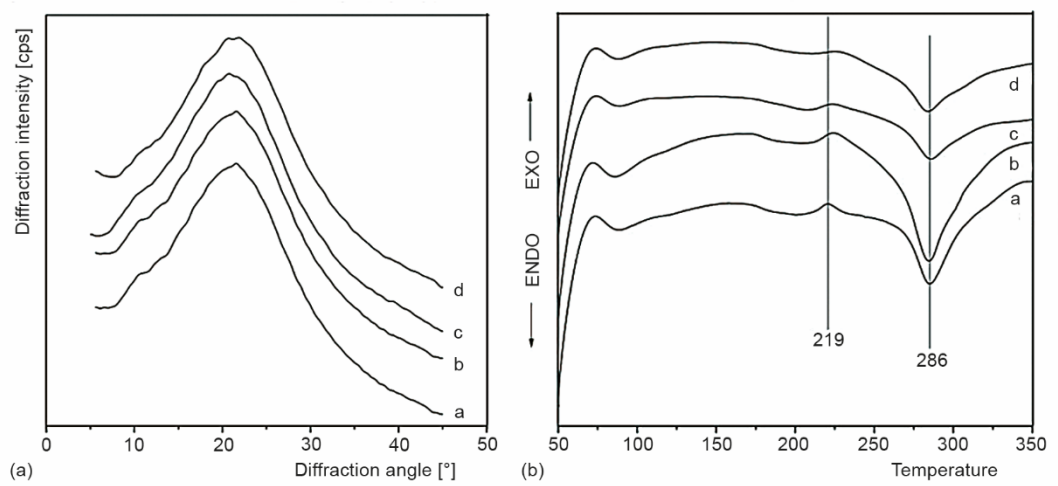

Figure 4. The XRD and DSC curves of c-SF scaffolds with reaction SF concentration; (a) 1%, (b) 2%, (c) 3%, and (d) 4%

Conclusion

The SF scaffolds were enzymatic cross-linked effectively by tyrosinase though the reaction between tyrosine and aminogroups of SF to form inter- and intra-molecular covalent bonds. The water resistance of c-SF scaffolds was improved significantly after cross-linking when the reaction ratios of TYR/SF was higher than 1/2000. The structure of c-SF scaffolds did not change obviously regardless of SF concentration, remaining the α-helix and random coil structure. Moreover, the average pore size of c-SF scaffolds was in range of 46-101 μm and porosity in range of 41%-60%. The pore size was changed to be smaller with the increase of SF concentration. These results revealed that tyrosinase as agent could induce self-cross-linking of SF, and the pore structure of SF scaffolds could be regulated by adjusting the reac-

tion SF concentration, and the thermal stability of SF scaffolds can be adjusted by porosity as discussed in [20, 21].

This paper proposes an effective approach to preparation of SF materials by the enzymatic cross-linking, and it provides tissue engineering with a promising opportunity of optimal design of a needed SF material, and its thermal and chemical and mechanical properties can be adjusted through the tyrosinase concentration, and the fractal approach [22, 23] to the theoretical analysis is a future research frontier.

Acknowledgment

This work was supported by the National Nature Science Foundation of China (51403146), Nature Science Foundation of Jiangsu Province (BK20161288, BK20191191) and Priority Academic Program Development of the Jiangsu Higher Education Institutions.

References

[1] Luo, T. T., *et al.*, Stabilization of Natural Antioxidants by Silk Biomaterials, *ACS Applied Materials & Interfaces, 8* (2016), 21, pp. 13573-13582
[2] Tian, D., *et al.*, Macromolecular-Scale Electrospinning: Controlling Inner Topologic Structure Through a Blowing Air, *Thermal Science, 26* (2022), 3B, pp. 2663-2666
[3] He, J. H., *et al.*, The Maximal Wrinkle Angle During the Bubble Collapse and Its Application to the Bubble Electrospinning, *Frontiers in Materials, 8* (2022), Feb., 800567
[4] Yao, D., *et al.*, Viscoelastic Silk Fibroin Hydrogels with Tunable Strength, *Acs Biomaterials Science & Engineering, 7* (2021), 2, pp. 636-647
[5] Alizadehgiashi, M., *et al.*, Multifunctional 3D-Printed Wound Dressings, *ACS Nano*., *15* (2021), 7, pp. 12375-12387
[6] Zawani, M., *et al.*, Injectable Hydrogels for Chronic Skin Wound Management: A Concise Review, *Biomedicines, 9* (2021), 5, 527
[7] Liu, L. G., *et al.*, Dropping in Electrospinning Process: A General Strategy for Fabrication of Microspheres, *Thermal Science, 25* (2021), 2B, pp. 1295-1303
[8] Yin, S., *et al.*, Hydrogels for Large-Scale Expansion of Stem Cells, *Acta Biomaterialia*, *128* (2021), July, pp. 1-20
[9] Li, X., *et al.*, Freezing-Induced Silk I Crystallization of Silk Fibroin, *Crystengcomm*, *22* (2020), 22, pp. 3884-3890
[10] Xue, R. J., *et al.*, A Fractional Model and Its Application to Heat Prevention Coating with Cocoon-Like Hierarchy, *Thermal Science, 26* (2022), 3B, pp. 2493-2498
[11] Optveld, R. C., *et al.*, Design Considerations for Hydrogel Wound Dressings: Strategic and Molecular Advances, *Tissue Engineering Part B-Reviews, 26* (2020), 3B, pp. 230-248
[12] Qian, M. Y., *et al.*, Collection of Polymer Bubble as a Nanoscale Membrane, *Surfaces and Interface, 28* (2022), Feb., 101665
[13] Huang, L., *et al.* Antheraea Pernyi Silk Fibroin-Coated Adenovirus as a VEGF165-Ang-1 Dual Gene Delivery Vector, *Journal of Bioactive and Compatible Polymers, 3* (2022), 3, pp. 189-204
[14] Xie, X. S., *et al.*, Prepration and Properties of Silk Fibroin Hydrogel for Biological, *Journal of Thermal Science, 26* (2022), 3B, pp. 2797-2804
[15] Chelazzi, D., *et al.*, Self-Regenerated Silk Fibroin with Controlled Crystallinity for the Reinforcement of Silk, *Journal of Colloid and Interface Science, 576* (2020), Sept., pp. 230-240
[16] Liu, X. P., *et al.*, Preparation of Thermosensitive Hydroxybutyl Chitosan/Silk Fibroin Hybrid Hydrogels, *Macromolecular Materials and Engineering, 307* (2022), 11, 220415
[17] Xue, R. J., *et al.*, Tussah Cocoon's Biomechanism: Fractal Insight and Experimental Verification, *International Journal of Thermal Sciences, 169* (2021), Nov., 107089
[18] Jiangseubchatveera N., *et al.*, The Evaluation of Antioxidant and Antityrosinase Efficacy of Carissa Carandas Fruit Extracts and the Development of a Preliminary Skincare Product, *Journal of Applied Pharmaceutical Science, 11* (2021), 7, pp. 153-157
[19] Wu, J. B., *et al.*, Oral Delivery of Curcumin Using Silk Nano- and Microparticles, *Acs Biomaterials Science & Engineering, 4* (2018), 11, pp. 3885-389

[20] Liu, F. J., *et al.*, Thermal Oscillation Arising in a Heat Shock of a Porous Hierarchy and Its application, *Facta Universitatis Series: Mechanical Engineering, 20* (2022), 3, pp. 633-645
[21] He, C. H., *et al*., A Fractal Model for the Internal Temperature Response of a Porous Concrete, *Applied and Computational Mathematics, 21* (2022), 1, pp. 71-77
[22] Zuo, Y.-T. and Liu, H.-J., Fractal Approach to Mechanical and Electrical Properties of Graphene/Sic Composites, *Facta Universitatis-Series Mechanical Engineering, 19* (2021), 2, pp. 271-284
[23] He, C. H., Liu, C., Fractal Dimensions of a Porous Concrete and Its Effect on the Concrete's Strength, *Facta Universitatis Series: Mechanical Engineering*, On-line first, https://doi.org/10.22190/FUME 221215005H, 2023

Paper submitted: December 25, 2022
Paper revised: March 17, 2023
Paper accepted: March 18, 2023